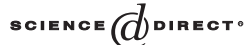


Available online at www.sciencedirect.com



DISCRETE APPLIED MATHEMATICS

Discrete Applied Mathematics 147 (2005) 265-285

www.elsevier.com/locate/dam

Expanding selfsimilar solutions of a crystalline flow with applications to contour figure analysis

Hidekata Hontani^a, Mi-Ho Giga^b, Yoshikazu Giga^b, Koichiro Deguchi^c

^aDepartment of Informatics, Yamagata University, Yonezawa, Yamagata, 992-8510, Japan
^bDepartment of Mathematics, Hokkaido University, Sapporo, Hokkaido, 060-0810, Japan
^cDepartment of System Information Sciences, Graduate School of Tohoku University, Sendai, 980-8579, Japan

Received 11 December 2003; received in revised form 19 May 2004; accepted 3 September 2004

Available online 28 December 2004

Abstract

A numerical method for obtaining a crystalline flow starting from a general polygon is presented. A crystalline flow is a polygonal flow and can be regarded as a discrete version of a classical curvature flow. In some cases, new facets may be created instantaneously and their facet lengths are governed by a system of singular ordinary differential equations (ODEs). The proposed method solves the system of the ODEs numerically by using expanding selfsimilar solutions for newly created facets. The computation method is applied to a multi-scale analysis of a contour figure. © 2004 Elsevier B.V. All rights reserved.

Keywords: Crystalline flow; Selfsimilar solutions; Evolving polygon; Multi-scale analysis

1. Introduction

A curvature flow is widely used for a multi-scale analysis of a contour figure in an image [1,15,18–20,22,24,27]. A curvature flow is a family of evolving contours, in which every point of the contour moves toward its normal direction with the velocity that is determined by the curvature. Fig. 1 shows an example of a curvature flow, in which the normal velocity is equal to the curvature. This flow is called a curve shortening flow. As a contour evolves, local details in the contour are smoothed out, and it is proved that, in a curve shortening

E-mail address: Hontani@yz.yamagata-u.ac.jp (H. Hontani).



Fig. 1. An example of a curve shortening flow.

flow, any simple closed curve becomes convex in finite time, and shrinks to a point; the way of shrinking is asymptotically close to that of a shrinking circle. A method for a multiscale analysis, in general, specifies a shape component from a given contour and finds each component's size by observing how the contour shape becomes close to a circle in the flow. The method records the time at which each shape component disappears in the flow for finding its size.

In many cases, a contour figure in an image is described as a polygon. In a curve shortening flow, it is proved that any given simple polygon becomes an analytic curve immediately after it starts evolving. Several methods have been proposed for computing the flow, and those methods usually describe an evolving smooth contour in a discrete way.

The Gaussian-based method [22], for example, describes an evolving contour figure by a set of points that are equally spaced in the contour. The coordinates of the *i*th point are represented as $(x(i\Delta), y(i\Delta))$ where Δ denotes the interval between adjacent points. The method iterates two processes: (i) smoothing both x and y with a small scale Gaussian filter, and (ii) resampling the resulted contour at equal intervals after the smoothing. The resampling process is needed because the arc length changes as the contour evolves. It should be noted that the interval Δ of the resampling changes at each iteration because Δ must aliquot of the total peripheral length, but it is not realizable. These things make it difficult to compute a curve shortening flow precisely. In addition, the resampling process makes it difficult to track each point in the evolving contour through the process. Many multi-scale methods needs to track a point in the evolving contour for finding the time at which a shape component disappears, therefore, such a resampling process is not desirable.

A level set method [5,6,23] is a powerful tool for obtaining an evolving interface. The method represents an evolving interface as the zero level set of an auxiliary function ϕ . For example, an evolving contour in the x-y plane is represented as the zero level set of the evolving function $\phi(x, y; t)$. To compute the curve shortening flow, we only need to solve the level set equation $\phi_t + \kappa |\nabla \phi| = 0$. Because no arc length parameter along the contour is needed for computation, no resampling along the contour is needed. Moreover, the method can compute an evolving interface even if its topology changes as it evolves. In the computation, though, the function ϕ is discretely represented on fixed pixels, and finite difference operators are used for computing the spatial derivatives. The operators' width is usually two or three pixels. If there exists a small part in the evolving contour that is comparable to the operators' width, then, the computed values do not approximate well the spatial derivatives. This inaccuracy causes a serious problem to compute the accurate value of the curvature κ . Unless we know the accurate value of κ , it is, for example, difficult to

choose inflection point of an evolving curve, which is important in a multi-scale contour figure analysis (see, e.g. [15,18,19,22,24,27]).

In [2,26], a crystalline flow is proposed to analyze motion of crystals in material sciences. A crystalline flow is a special family of evolving polygons, which is often called an admissible evolving crystal. It can be regarded as a discrete version of a curvature flow. In an evolving process of the crystalline flow, a given polygon remains polygonal through the evolving process, each facet (side) of evolving contour moves keeping its normal direction, and every corner in the contour moves at least C^1 in time (provided that no facets disappear). These features help to track each facet through the evolving process, so that the flow is useful for the multi-scale analysis. The velocity is determined by the non-local curvature, which depends on the length of the facet. Polygons are well represented in a discrete manner. Different from a classical curvature flow, it is easy to compute the accurate value of non-local curvature, and to obtain the crystalline flow if an appropriate initial polygon is given.

As already observed in [2,26], a crystalline flow can be interpreted as a curvature flow with anisotropic interfacial energy density. The governing equation is formally written as a partial differential equation (PDE) of the second order: like a curve shortening equation. However, the quantity like nonlocal curvature is not an infinitesimal quantity, so it is not a conventional PDE. In [3], a nonlinear partial differential equation is obtained from dilation and erosion processes. However, the PDE derived in [3] is of the first order and anisotropy arises in the first-order term; see also [25]. The effect of the anisotropy obtained by a crystalline arises in the curvature term and is quite different from the anisotropy of [3,25]. For relations of morphological operations and curvature effects, the reader is referred to a recent book of Cao [4].

In [2,26], evolving curves for crystalline flow are restricted in a special class of evolving polygons. In particular, only a special polygon is allowed to be an initial data. In [9,10], a level set formulation was extended to handle a curvature flow with singular interfacial energy, including a crystalline flow. Moreover, one is allowed to take an arbitrary curve as initial data for unique global-in-time solvability[10]. However, its explicit form was not clear even if an initial data is a polygonal contour. In some cases, new facets are expected to be created at corners of a given polygon instantaneously. Once new facets are created, no new facet is created any more, and the number of facets decreases monotonically as time increases, unless evolving polygon degenerates. It turns out that if the speeds of both facets bounding newly created facets are zero, then these new facets expand selfsimilarly, and their lengths solve a system of singular ordinary differential equations. The unique existence of such a selfsimilar solution has been established by solving a system of algebraic equations [11,12]. (The explicit values of the solution is not given in [11,12].) We summarise this result in Section 2, while in 3, we give a numerical way to find selfsimilar expanding solutions. In Section 2, we introduce a new notion 'essential admissible crystal' which is a slight extension of 'admissible crystal (polygon)' in [2,26], to treat general initial polygon.

In this paper, we present a numerical method to obtain a crystalline flow from *arbitrary* given polygon. A numerical length of each newly created facet is calculated by using the expanding selfsimilar solution. The proposed method enables us to use any convex polygon as the Wulff shape, which controls the nonlocal curvature of each facet. The Wulff shape substitutes the disk in the sense that its nonlocal curvature is constant. If the Wulff shape

is different, then the crystalline flow is also different for the same initial data (Fig. 9). In particular, if we rotate the Wulff shape, the flow may be different. However, approximating the disk by a polygonal Wulff shape, one is able to approximate a curve shortening flow (which is rotationally invariant) by a crystalline flow (see, e.g. [10]).

In this paper, we apply the proposed method for computing the crystalline flow to extracting a set of dominant facets from a given contour figure. As mentioned above, in the crystalline flow, it is easy to track each facet through the process; in particular, it is easy to distinguish convex part, concave part, and inflection part of evolving polygons. The proposed method tracks each facet in a given polygon through the evolving process, and extracts facets that remain existing for a long time. In [16], the first and the last authors firstly applied a crystalline flow to a multi-scale contour figure analysis. However, the proposed method in [16] did not create new facets systematically. To overcome this inconvenience, in this paper, the length of each new facet is approximated by expanding selfsimilar solutions obtained in [11,12]. Note that our method does not include any approximation error caused by spatial grid size, which is an advantage over finite difference method for calculating curvature flows.

This paper is organized as follows: In Section 2, we outline mathematical backgrounds of a crystalline flow with expanding selfsimilar solutions, which may appear as newly created facets. In Section 3, we present a numerical method for computing a crystalline flow. Sections 4 and 5 show some experimental results and conclusions, respectively. A preliminary version of this paper has been published in [17].

2. Crystalline flow

2.1. Weighted curvature flow

First, we recall the notion of the weighted curvature. Let γ be a continuous, convex function on \mathbb{R}^2 which is positively homogeneous of degree one, i.e., $\gamma(\lambda p) = \lambda \gamma(p)$ for all $p \in \mathbb{R}^2$, $\lambda > 0$. Assume that $\gamma(p) > 0$ for $p \neq 0$. For a moment assume that γ is smooth (except the origin). Fig. 2 shows an example of the graph of $\gamma(p)$. For an oriented curve S with the orientation n, which is a unit normal, we call $\Lambda_{\gamma}(n) = -\text{div}(\xi(n))$ the weighted curvature of S in the direction of n, where $\xi = \nabla \gamma$. We note that the weighted curvature of S is the first variation of I(S) with respect to a variation of the area enclosed by S; here I(S) is defined by

$$I(S) = \int_{S} \gamma(\mathbf{n}) \, \mathrm{d}s,\tag{1}$$

where ds denotes the line element; I(S) is called the *interfacial energy* with an *interfacial energy density* γ . We recall that the Wulff shape defined by

$$W_{\gamma} = \bigcap_{|\boldsymbol{m}|=1} \{ \boldsymbol{x} \in \boldsymbol{R}^2; \boldsymbol{x} \cdot \boldsymbol{m} \leqslant \gamma(\boldsymbol{m}) \}$$

is the unique minimizer of I(S) among all S whose enclosed area is the same as W_{γ} (see, e.g. [14]). If $\gamma(\mathbf{p}) = |\mathbf{p}|$, then I(S) is equal to the total peripheral length of S, Λ_{γ} is the

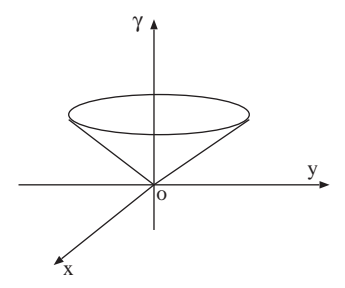


Fig. 2. Interfacial energy density γ .

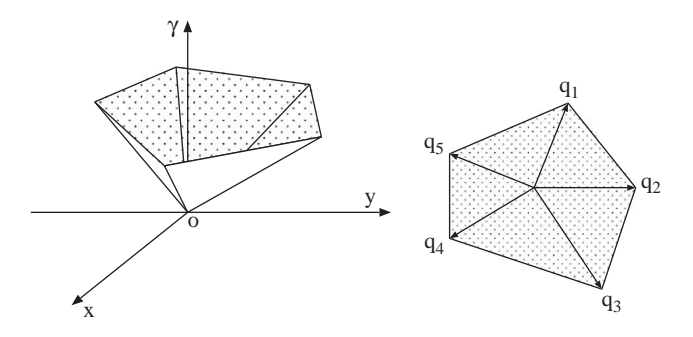


Fig. 3. Crystalline energy density and its Frank diagram.

usual curvature, and W_{γ} is nothing but a unit disk. For any γ the weighted curvature of ∂W_{γ} always equals -1, so W_{γ} plays the role of a unit disk for the usual curvature.

We consider a motion of an evolving curve Γ_t governed by the *anisotropic curvature* flow equation of the form

$$V = \Lambda_{\nu}(\mathbf{n}) \tag{2}$$

on Γ_t , where V denotes the normal velocity of $\{\Gamma_t\}$ in the direction of \boldsymbol{n} . When $\gamma(\boldsymbol{p}) = |\boldsymbol{p}|$, Eq. (2) becomes the curve shortening equation.

There are several methods to track evolution of Γ_t ; one of a typical method is the level-set method (see [5–7,23]). If γ is C^2 except the origin, global unique solvability for (2) is established by Chen et al. [5] (see also [13]). However, when γ has corners, conventional notion of a solution including viscosity solutions does not apply to (2).

If Frank diagram of γ :

Frank
$$\gamma = \{ \boldsymbol{p} \in \boldsymbol{R}^2; \gamma(\boldsymbol{p}) \leq 1 \}$$

is a convex polygon, γ is called a *crystalline energy (density)* (see Fig. 3), and a notion of solution for (2) is proposed by Angenent and Gurtin [2] and Taylor [26] independently by restricting $\{\Gamma_t\}$ as a special family of evolving polygonal curves called admissible. Even for more general γ with corners not necessarily crystalline energy, the level-set approach

for (2) and more general equations is successfully extended by Giga and Giga [10] (see also [9]), although the problem has nonlocal nature. They introduced a new notion of solution consistent with that in [2,26], and proved the global unique solvability at least for a *general* initial simple curve (not necessarily admissible). However, for a general initial polygon, the explicit form of a solution was not discussed in [9,10] when γ is crystalline.

2.2. Crystalline flow

Here and hereafter we assume that γ is a crystalline energy, i.e., Frank γ is a convex M-polygon. In this section we introduce an evolving polygonal curve called a crystalline flow governed by (2). To track such an evolving polygon, we shall derive a system of ordinary differential equations (ODEs) for the length of sides (facets) of the polygon. For this purpose we need to prepare several notions.

Let q_i (i = 1, ..., M) be vertices of Frank γ as shown in Fig. 3. We call a simple oriented polygonal curve S as an *essentially admissible crystal* if the outward unit normal vector \mathbf{n} and $\hat{\mathbf{n}}$ of any adjacent segments (facets) of S satisfy

$$\frac{(1-\lambda)n + \lambda \hat{n}}{|(1-\lambda)n + \lambda \hat{n}|} \notin \mathcal{N}$$
(3)

for any $\lambda \in (0, 1)$, where $\mathcal{N} = \{q_i/|q_i|; i=1,\ldots,M\}$. Let J be a time interval. We say that a family of polygon $\{S(t)\}_{t\in J}$ is an essentially admissible evolving crystal if S(t) is an essentially admissible crystal for all $t\in J$ and each corner moves continuously differentiably in time. These conditions imply that the orientation of each facet is preserved in J. By definition S(t) is of the form $S(t) = \bigcup_{j=1}^r S_j(t)$ where $S_j(t)$ is a maximal, nontrivial, closed segment and its unit outward normal vector is \mathbf{n}_j . Here we number facets clockwise. Then we obtain a transport equation for $L_j(t)$ which is the length of $S_j(t)$:

$$\frac{\mathrm{d}L_j(t)}{\mathrm{d}t} = (\cot \psi_j + \cot \psi_{j+1})V_j - \frac{1}{\sin \psi_j}V_{j-1} - \frac{1}{\sin \psi_{j+1}}V_{j+1}$$
(4)

for j = 1, ..., r; index j is considered modulo r. Here $\psi_j = \theta_j - \theta_{j-1}$ (modulo 2π) with $n_j = (\cos \theta_j, \sin \theta_j)$, and V_j denotes the normal velocity of $S_j(t)$ in the direction of n_j . We say that an essentially admissible crystal $\{S(t)\}_{t \in J}$ is a γ -regular flow of (2) if

$$V_j(t) = \chi_j \frac{\Delta(\mathbf{n}_j)}{L_j(t)} \tag{5}$$

for $j=1,2,\ldots,r$. Here $\Delta(\mathbf{n}_j)=\tilde{\gamma}'(\theta_j+0)-\tilde{\gamma}'(\theta_j-0)$ with $\mathbf{n}_j=(\cos\theta_j,\sin\theta_j)$ and $\tilde{\gamma}(\theta)=\gamma(\cos\theta,\sin\theta)$. We note that $\Delta(\mathbf{n}_j)$ is the length of facet of W_γ with outward normal \mathbf{n}_j if $\mathbf{n}_j\in\mathcal{N}$ (see Fig. 4), otherwise $\Delta(\mathbf{n}_j)=0$. The quantity χ_j is called a transition number, and takes +1 (resp. -1) if S(t) is concave (resp. convex) around jth facet in the direction of \mathbf{n}_j , otherwise $\chi_j=0$. We call the quantity $\Lambda_j\equiv\chi_j\Delta(\mathbf{n}_j)/L_j(t)$ as a nonlocal weighted curvature of the jth facet with respect to γ . (We use the convention that $1/L_j(t)=0$ if $L_j(t)=\infty$.) Thus we get a system of ODEs (4) and (5) for $L_j(t)$'s. For a moment we assume that S(0) is an essentially admissible closed curve, that is to say, a closed curve which is an essentially admissible crystal.

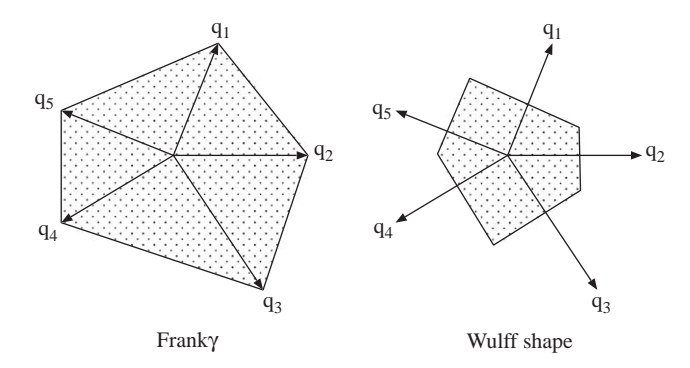


Fig. 4. Frank γ and the corresponding Wulff shape. Each facet of the Wulff shape has the length $\Delta(m_i)$, where $m_i = q_i/|q_i|$.

A fundamental theory of ODE yields the (local in time) unique solvability of (4) and (5). Unless S(t) shrinks to a point, self-intersects, or develops degenerate pinching at most two consecutive facets with zero nonlocal weighted curvatures may disappear (i.e., the length of a facet tends to zero) at some time T_* . However, $S(T_*)$ remains essentially admissible, so that we can continue calculating the ODE system (4),(5) for $t > T_*$ starting with initial data $S(T_*)$ (see [26,9]).

We say that $\{S(t)\}_{t\in J}$ is a *crystalline flow* with initial data S(0), if there is some $t_0=0 < t_1 < t_2 < \cdots < t_l$, such that $\{S(t)\}_{t\in J_h}$ is a γ -regular flow for $J_h = [t_h, t_{h+1})$ with initial data $S(t_h)$ $(h=0,1,\ldots,l-1)$, and $S(t) \to S(t_{h+1})$ in the sense of the Hausdorff distance topology as $t \uparrow t_{h+1}$ and some facets disappear at t_{h+1} $(h=0,1,\ldots,l-2)$. By a similar argument as in [9], we see that a crystalline flow $\{S(t)\}_{t\in J}$ starting with essentially admissible closed curve S(0) shrinks to a point and does not intersect nor develop degenerate pinching provided that W_{γ} is rotationally symmetric with respect to some point. A crystalline flow $\{S(t)\}_{t\in J}$ agrees with a solution by level-set approach for (2) introduced in [10], by a similar argument as in [9] (see also [8]). The discussion in [9] is for an admissible evolving crystal but it is easy to extend to an essentially admissible evolving crystal. For convenience we recall the notion of an admissible evolving crystal. An essentially admissible crystal S(t) is called an *admissible crystal* if the outward unit normal vector \mathbf{m} of each segment of S(t) belongs to S(t) we say S(t) is an *admissible evolving crystal* if S(t) is an admissible crystal for each $t \in J$.

2.3. General polygonal initial curve

In the previous section we restricted an initial curve to an essentially admissible crystals. Here we shall focus on a simple, closed, polygonal initial curve S(0), which is not necessarily an essentially admissible crystal. In [10], it is shown that there exists a unique level-set flow (solution) for (2) with a crystalline energy γ starting with a general polygonal initial curve. However, it is not clear a priori whether or not the solution is described by an ODE system, since new facets whose orientation belongs to $\mathcal N$ are expected to be created instantaneously at the place where property (3) is violated on S(0). Moreover, it is not clear how to solve

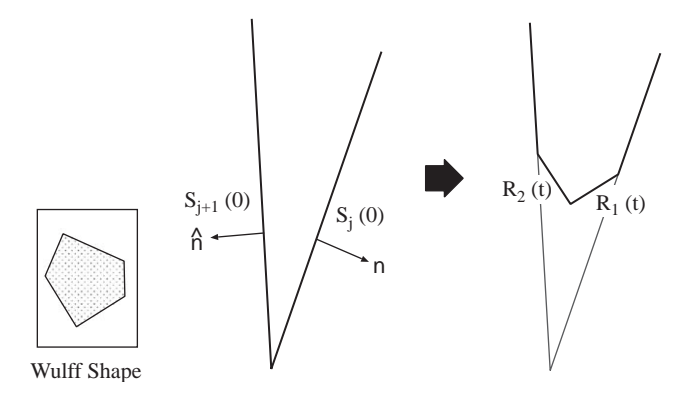


Fig. 5. Creation of a set of new facets. All facets with orientation in \mathcal{M} are expected to be created between $S_j(0)$ and $S_{j+1}(0)$ just after t=0. It should be noted that the length of each new facet should satisfy the ODE system of (4) and (5).

the expected ODE system since it is singular at newly created facets. In this section we give a heuristic argument to solve such a singular ODE system.

Let n and \hat{n} be the orientation of any adjacent facets $S_j(0)$ and $S_{j+1}(0)$ of S(0). If

$$\mathcal{M} \equiv \left\{ \frac{(1-\lambda)\boldsymbol{n} + \lambda \hat{\boldsymbol{n}}}{|(1-\lambda)\boldsymbol{n} + \lambda \hat{\boldsymbol{n}}|} \in \mathcal{N}; \quad 0 < \lambda < 1 \right\}$$

is not the empty set, all facets (say, $R_1(t), \ldots, R_n(t)$, numbered clockwisely) with orientation in \mathcal{M} are expected to be created between $S_j(0)$ and $S_{j+1}(0)$ just after t=0, so that the transition number of each $R_i(t)$ is 1 (resp. -1) for small t>0 if the bounded polygon enclosed by S(0) is concave (resp. convex) near $S_j(0) \cap S_{j+1}(0)$ (see Fig. 5). By inserting these newly created facets, our solution S(t) should become essentially admissible instantaneously. This observation should be justified by approximating S(0) by essentially admissible crystals from inside and from outside with comparison principle [10].

For a given initial polygon S(0) one is able to find the place, the orientation and the transition number of the all facets that are expected to be newly created at initial time. For later convenience, we shall re-number clockwisely all facets of S(0) and all facets that are expected to be created at t=0, i.e., the length of a newly created facet equals 0 at t=0. Then the expected ODE system for a simple, closed, polygonal initial curve S(0) again becomes (4) and (5); however, the initial data $L_i(0)$ may be 0. The ODE system is of the form

$$\frac{\mathrm{d}L_{j}(t)}{\mathrm{d}t} = \frac{\tilde{p}_{j}}{L_{j}(t)} + \frac{\tilde{q}_{j-1}}{L_{j-1}(t)} + \frac{\tilde{r}_{j+1}}{L_{j+1}(t)},\tag{6}$$

where $\tilde{p}_j = (\cot \psi_j + \cot \psi_{j+1})\chi_j \Delta(\boldsymbol{n}_j)$, $\tilde{q}_{j-1} = -\chi_{j-1}\Delta(\boldsymbol{n}_{j-1})/\sin \psi_j$, and $\tilde{r}_{j+1} = -\chi_{j+1}\Delta(\boldsymbol{n}_{j+1})/\sin \psi_{j+1}$ for $j=1,\ldots,r'$; index j is considered modulo r'. Here numbers \tilde{p}_j , \tilde{q}_j , \tilde{r}_j are determined uniquely by (4) and (5), since the transition number and the orientation of a newly created facet are known.

To solve Eq. (6) we consider Puiseux series

$$L_{j}(t) = \sum_{k=0}^{\infty} a_{jk} t^{k/2},\tag{7}$$

with real number a_{jk} . Clearly, for j with $L_j(0)=0$ the coefficient a_{j0} must be zero. Suppose that n consecutive facets, say $S_1(t),\ldots,S_n(t)$ are created at t=0, i.e. $L_1(0)=\cdots=L_n(0)=0$ and $L_0(0),L_{n+1}(0)>0$. We plug (7) into (6) and multiply $t^{1/2}$ with both sides of (6). Comparing both sides we observe that all coefficients are determined. The first coefficients $\{a_{j1}\}_{j=1}^n$ have a significant meaning. If the nonlocal curvature of $S_0(0)$ and $S_{n+1}(0)$ equals zero, then $L_j(t)=a_{j1}t^{1/2}$ for $j=1,\ldots,n$ exactly solves the ODE system (6) with $j=1,\ldots,n$ (as long as both $S_0(t)$ and $S_{n+1}(t)$ exist), since it is decoupled from the whole system (6) with $j=1,\ldots,r'$ by the fact $\tilde{q}_0=0=\tilde{r}_{n+1}$. In this case the solution $\{a_{j1}\}_{j=1}^n$ represents a selfsimilar expanding solution of the problem in the next section.

2.4. Selfsimilar expanding solutions

Let $\{S(t)\}_{t>0}$ be an essentially admissible evolving crystal of the form $S(t) = \bigcup_{j=0}^{n+1} S_j(t)$ with nonparallel half lines $S_0(t)$ and $S_{n+1}(t)$. We say that $\{S(t)\}_{t>0}$ is *selfsimilar* if there exists an essentially admissible crystal S_* such that

$$S(t) = t^{1/2} S_* = \{t^{1/2} x; x \in S_*\}, \quad t > 0.$$

If $\{S(t)\}_{t>0}$ solves (6), we call $\{S(t)\}_{t>0}$ a *selfsimilar expanding solution* of (2). By definition $S(+0) = \lim_{t \downarrow 0} S(t)$ consists of two (nonparallel) half lines emanated from the origin. We also observe that $\bigcup_{j=1}^n S_j(t)$ is admissible for all t>0 and that the transition number of $S_j(t)$ is independent of $j=1,\ldots,n$ and t>0; it must be either -1 or +1. It turns out that $\{S(t)\}_{t>0}$ is a selfsimilar expanding solution if and only if the length $L_j(t)$ of $S_j(t)$ $(j=1,\ldots,n)$ solves the ODE system (6) for t>0 and for $j=1,\ldots,n$ with $\tilde{q}_0=0=\tilde{r}_{n+1}$. Note that a_{j1} of $L_j(t)=a_{j1}t^{1/2}$ represents the length of jth facet of S_* for $j=1,\ldots,n$.

Theorem 1. For a given oriented closed cone C (with connected interior) there exists a unique selfsimilar expanding solution S(t) such that S(+0) agrees with the boundary of C (see [11,12]).

From ODE system (6) we see that this problem is equivalent to the unique solvability of algebraic equation

$$\begin{bmatrix} a_{n} \\ a_{n-1} \\ a_{n-2} \\ \vdots \\ a_{2} \\ a_{1} \end{bmatrix} = 2 \begin{bmatrix} \tilde{p}_{n} & \tilde{q}_{n-1} \\ \tilde{r}_{n} & \tilde{p}_{n-1} & \tilde{q}_{n-2} & 0 \\ & \tilde{r}_{n-1} & \tilde{p}_{n-2} & \tilde{q}_{n-3} \\ & & \ddots & \ddots & \ddots \\ & 0 & & \tilde{r}_{3} & \tilde{p}_{2} & \tilde{q}_{1} \\ & & \tilde{r}_{2} & \tilde{p}_{1} \end{bmatrix} \begin{bmatrix} 1/a_{n} \\ 1/a_{n-1} \\ 1/a_{n-2} \\ \vdots \\ 1/a_{2} \\ 1/a_{1} \end{bmatrix}$$
(8)

for $a_j = a_{j1} > 0$ (j = 1, 2, ..., n). We proved the existence of a solution of this algebraic equation by a method of continuity while we proved its uniqueness by a geometric observation [11,12].

3. Numerical method for obtaining a crystalline flow

In this section, we describe a numerical method for obtaining a crystalline flow starting from a given polygon that is not necessarily an essentially admissible crystal. Using the Euler method, we compute the approximated solution of the system of (4) and (5). If the given polygon is not essentially admissible, our method firstly creates new facets. When the new facets are created, the length of any facet in a given polygon is not updated. After the new facets are created, then we update the lengths of all facets to compute the approximated solution.

3.1. New facet creation

For each adjacent facets with orientation m and \hat{m} of the initial polygon, if $\mathcal{M} \neq \emptyset$ then all facets with orientation in \mathcal{M} should be newly created instantaneously, so that the given polygon becomes essentially admissible instantaneously. Once the polygon becomes essentially admissible, no new facet is needed to be created.

Given a nonessentially admissible polygon, the method creates new facets at first time. For creating new facets, we should numerically calculate the solution of (8) in order to obtain the lengths of them. Let the time step be denoted as Δt . We set the length of each new facet to $a_i \sqrt{\Delta t}$, where a_i is a numerical solution of (8).

To solve (8) numerically, as in [11,12] we rewrite (8) with $\alpha_i = 1/a_i$:

$$\begin{bmatrix} 1/\alpha_{n} \\ 1/\alpha_{n-1} \\ \vdots \\ 1/\alpha_{2} \\ 1/\alpha_{1} \end{bmatrix} = H_{n} \begin{bmatrix} \alpha_{n} \\ \alpha_{n-1} \\ \vdots \\ \alpha_{2} \\ \alpha_{1} \end{bmatrix}, \quad \text{where } H_{n} = \begin{bmatrix} p_{n} & q_{n-1} \\ r_{n} & p_{n-1} & q_{n-2} & 0 \\ & \ddots & \ddots & \ddots \\ 0 & & r_{3} & p_{2} & q_{1} \\ & & & r_{2} & p_{1} \end{bmatrix}, \quad (9)$$

where $p_j = 2\tilde{p}_j$, $q_j = 2\tilde{q}_j$, and $r_j = 2\tilde{r}_j$. We introduce extra parameter $s \in [0, 1]$ by replacing H_n by $K_n(s)$ in (9) so that α_j depends on s.

$$K_n(s) = \begin{bmatrix} p_n & sq_{n-1} \\ sr_n & p_{n-1} & sq_{n-2} & 0 \\ & \ddots & \ddots & \ddots \\ 0 & & sr_3 & p_2 & sq_1 \\ & & & sr_2 & p_1 \end{bmatrix}.$$
(10)

Evidently $[1/\alpha_j(0)] = K_n(0)[\alpha_j(0)]$ can be easily solved, and $\{\alpha_j(1)\}_{j=1}^n$ is the solution of (9): $\alpha_j(0) = 1/\sqrt{p_j}$. Referring the idea of [11,12], we calculate the numerical solution

of (9) using the Newton-Rapson method as follows.

- (1) Set $\alpha_i = 1/\sqrt{p_i}$ for initial values of the iteration, where $p_j = 2[\cot \psi_i + \cot \psi_{i+1}]\chi_i \Delta(\mathbf{n}_j)$.
- (2) Apply the Newton–Rapson method to obtain the numerical solution of α_j .

Finally, we calculate $a_j = 1/\alpha_j$, and set the length of each new facet to $a_j \sqrt{\Delta t}$. Note that $L_j(t) = a_j t^{1/2}$ is the exact solution if the velocities of both facets bounding newly created facets are zero. The polygon obtained by the new facet creation is expected to approximate well the solution of the system of (4) and (5) corresponding to $t = \Delta t$, though we have not proved it rigorously.

3.2. Computing crystalline flow

As described in the previous subsection, if a given polygon is not essentially admissible, then the new facets are created. The resulted polygon is essentially admissible. Given the Wulff shape and a simple initial polygon, our method computes the solution of the system of (4) and (5) using the Euler method.

- (1) Create new facets as described in the previous subsection, if a given initial polygon is not essentially admissible. The length of a facet in the given polygon is not updated in this step.
- (2) Update the length of every facet in the polygon as $L_j(t_0 + \Delta t) = L_j(t_0) + \Delta t \cdot dL_j(t)/dt|_{t=t_0}$.
- (3) Iterate step (2) till the polygon becomes convex, or some facet with $\chi = \pm 1$ becomes smaller than a prescribed value, say $\varepsilon_0 > 0$.

Note that the evolving polygon becomes convex provided that the Wulff shape is rotationally symmetric with respect to some point [9].

4. Experimental results

4.1. Computation of a crystalline flow

In the first experiment, we used a regular 16-polygon as the Wulff shape, and a sector as an initial contour as shown in Fig. 6. Let m_i ($i=1,2,\ldots,16$) denote the outward unit normals of the Wulff shape; the facet number i is indexed clockwisely. We set that the argument of m_i equals $\pi - \pi(i-1)/8$. Let S_j denote the jth facet of the initial contour, and n_j (j=1,2,3,4) be the outward unit normal of S_j . Assume that arg $n_j = \pi - \pi(j-1)/2$. Then, three new facets sprout out at each corner of the square. For example, between S_1 (arg $n_1 = \pi$) and S_2 (arg $n_2 = \pi/2$) of the given square, three facets sprout out of which normals are parallel to m_2 , m_3 , and m_4 , respectively. We note that n_1 (resp. n_2) of the sector (A) in Fig. 7 equals m_1 (resp. m_5). However, the weighted curvatures of two half lines S_1 and S_2 are zero, since the length of S_1 and S_2 is infinite.

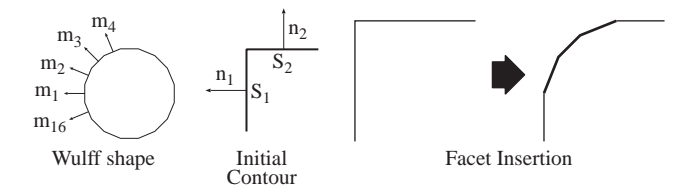


Fig. 6. An example of the Wulff shape and an initial contour. An analytic solution can be calculated in this case. Three new facets are created at the beginning as shown in this figure. It should be noted that the middle facet is shorter than side ones.

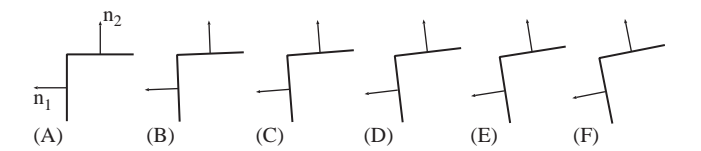


Fig. 7. An example of the set of given rotated sectors. The arguments of n_1 are (A) π , (B) $\pi + \pi/80$, (C) $\pi + 2\pi/80$, (D) $\pi + 3\pi/80$, (E) $\pi + 4\pi/80$, and (F) $\pi + 5\pi/80$, respectively.

In order to obtain the quantities of a_i , we solve next equations that correspond to (8).

$$\begin{bmatrix} a_4 \\ a_3 \\ a_2 \end{bmatrix} = \begin{bmatrix} p & q & 0 \\ q & p & q \\ 0 & q & p \end{bmatrix} \begin{bmatrix} 1/a_4 \\ 1/a_3 \\ 1/a_2 \end{bmatrix},$$
where $p = 4/\tan(\pi/8)$ and $q = -2/\sin(\pi/8)$. (11)

Let $\alpha = 1/a_2 = 1/a_4$ and $\beta = 1/a_3$. Eq. (11) can be solved analytically:

$$\alpha = -(p\beta - 1/\beta)/2q,$$

$$\beta = \left[(p^2 + q^2) + \sqrt{(p^2 + q^2)^2 - p^2(p^2 - 2q^2)} \right]^{1/2} / \left[p(p^2 - 2q^2) \right]^{1/2}. \quad (12)$$

We can calculate the quantities a_j 's using $a_2 = a_4 = 1/\alpha$ and $a_3 = 1/\beta$. The values p and q in (12) are known as shown in (11). The values are $a_2 = a_4 \simeq 1.68$ and $a_3 \simeq 1.29$, respectively. Three facets sprout out with symmetric shape in this case. It should be noted that the shape of newly created facets is not the same as the shape of the corresponding part of the Wulff shape. In this case, the middle facet is shorter than the neighbours, although the Wulff shape is regular. Table 1 (A) shows the quantities a_j 's of Eq.(11) computed numerically by the method described in Section 3.1. The computed quantities well approximate the solution.

If a given initial contour is rotated, then the shape of new facets changes. We applied the proposed method for each sector shown in Fig. 7. The sector is rotated with increments of $\pi/80$. The length of each new facet is denoted by a_j . Table 1 shows the calculated values of a_j , which correspond to the new facets between S_1 and S_2 . In case of sector (A) three facets sprout out between S_1 and S_2 . On the other hand, for the other sectors four facets sprout out between S_1 and S_2 , because arg $n_1 < arg n_1$. Fig. 8 shows the shape of

	Ç					
	(A)	(B)	(C)	(D)	(E)	(F)
$Arg n_1$	π	$\pi + \pi/80$	$\pi + 2\pi/80$	$\pi + 3\pi/80$	$\pi + 4\pi/80$	$\pi + 5\pi/80$
$\text{Arg } n_2$	$\pi/2$	$\pi/2 + \pi/80$	$\pi/2 + 2\pi/80$	$\pi/2 + 3\pi/80$	$\pi/2 + 4\pi/80$	$\pi/2 + 5\pi/80$
a_1	_	5.891	3.924	3.090	2.614	2.303
a_2	1.682	1.464	1.382	1.326	1.286	1.257
a_3	1.287	1.232	1.223	1.225	1.287	1.257
a_4	1.682	1.719	1.806	1.925	2.085	2.303

Table 1 Experimental results obtained from the rotated sectors shown in Fig. 7

The numerically calculated solutions a_j are shown. The quantity $a_j \sqrt{\Delta t}$ represents the length of the newly created *i*th facet.

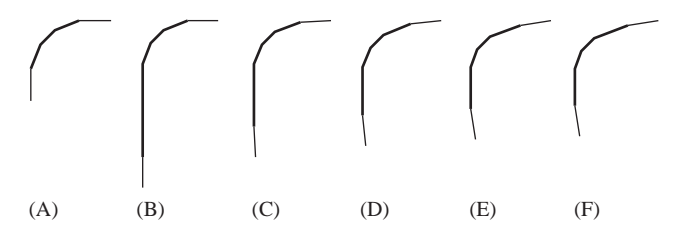


Fig. 8. The shape of new facets that correspond to Fig. 7 and Table 1. The thick lines indicate the new facets.

the new facets. For sector (B) the normal n_1 is almost parallel to the new facet's normal m_1 , and a_1 is large.

Fig. 9 shows some experimental results of crystalline flow. The initial contour is common to all, but the Wulff shape is different. As described earlier, the Wulff shape plays the role of a unit circle for a classical curve shortening flow. Because the proposed method gives a crystalline flow numerically from a non essentially admissible crystal, any simple and convex polygon can be used for the Wulff shape. A given initial contour becomes essentially admissible instantaneously, and since then no new facet is created. If the Wulff shape is rotationally symmetric with respect to some point, then any contour becomes convex in finite time [9].

4.2. Dominant facet extraction using a crystalline flow

As mentioned above, in a crystalline flow, any simple closed curve becomes convex at finite time, and it is easy to track each facet in the evolving contour. Those features of a crystalline flow are useful for a multi-scale analysis of a contour figure. In the following, we apply the crystalline flow to a multi-scale method that extracts dominant facets from a given polygon. The presented method is analogous to classical multi-scale methods for corner extraction (see, e.g. [24]).

In general, it is necessary to interact with a figure using some operators in order to detect features from it. The size of an operator is called a *scale*. An operator suppresses

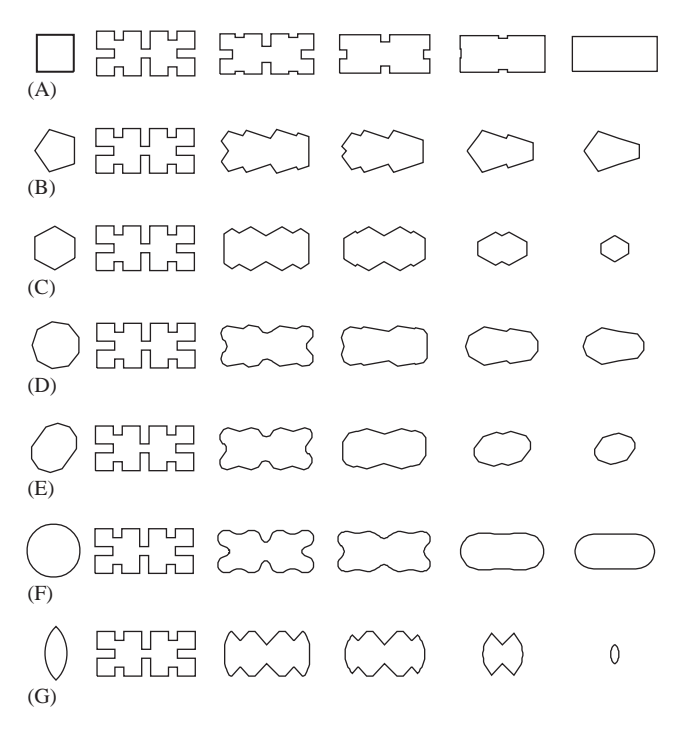


Fig. 9. Examples of the crystalline flow. The initial contour shown in the second column is common to all, and its evolution is shown from left to right. The Wulff shapes are shown in the left column: (A) a square, (B) a regular pentagon, (C) a regular hexagon, (D) a regular 9-polygon, (E) a 10-polygon which has two longer facets, (F) a regular 32-polygon, and (G) a 32-polygon in which each facet has same length.

features smaller than its scale, and detects features comparable in size to the scale [20]. To suppress small details, many multi-scale methods computes a curve shortening flow of a given contour. Those multi-scale methods interact with the evolving contour at every time using a small (fixed size) operator to detect features of the given contour at multiple scales. The time parameter t in a curve shortening flow represents the scale. Identical to a curve shortening flow, we regard the time parameter t in a crystalline flow as a scale parameter. The proposed method detects a shape feature at multiple scales by detecting the shape feature of three adjacent facets in the evolving polygon.

As mentioned in Section 2, each facet in an evolving polygon has a transition number χ , which represents the shape around the facet. It specifies whether the shape is convex, concave, or otherwise around the facet, which is a fundamental shape feature of a contour figure. If the shape is convex around some facet in a evolving polygon at some large scale, then we may interpret that the shape of the given contour is 'almost convex with small size disturbance' in a large area around the corresponding facet of the given contour. We call the facets in a given polygon whose transition numbers do not change through a long range of the scale in the crystalline flow as dominant facets.

In order to extract dominant facets, we make a scale-space representation [27] of a given polygon using a crystalline flow. The x-axis of the scale-space shows the indices j of early

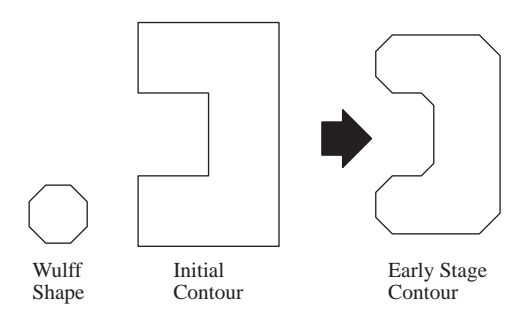


Fig. 10. An initial contour S(0) and the corresponding early stage contour $S(\tilde{t})$.

stage contour defined below, and the y-axis shows the time t. As time increases, each facet of the early stage contour moves, and is contained in some (nontrivial) facet in the evolved polygon S(t). The value of a point (j, t) in the scale-space shows the transition number of the facet in S(t) which includes the facet j in the early stage contour. Referring to this scale-space representation, the proposed method extracts dominant facets whose transition numbers are inherited for a long time interval in the evolving process.

Let us consider crystalline flow S(t) starting from initial contour S(0) which is a general simple polygon. As we mentioned in Section 2, some facets may be created at some corners spontaneously, so that the initial polygon becomes essentially admissible right after t = 0. As time evolves, no more facets are created other than at t = 0; however, at most two consecutive facets with zero transition number may disappear [8].

We say that $S(\tilde{t})$ is an *early stage contour* if no facet disappears and no degenerate pinching and no selfintersection occurs for all $t \in (0, \tilde{t}]$ (see Fig. 10). We index all facets of an early stage contour by $j = 1, 2, \ldots, r$, clockwisely. The totality of indices denotes \mathscr{I} ; we consider this set modulo r. We shall assign a subset $\mathscr{I}_h(t)$ of consecutive indices in \mathscr{I} to each facet $F_h(t)$ of $S(t) = \bigcup_{h=1}^k F_h(t)$ and divide \mathscr{I} into disjoint subsets $\{\mathscr{I}_h(t)\}_{h=1}^k$ in the following inductive way. We call $\mathscr{I}_h(t)$ the set of early stage indices of $F_h(t)$. Suppose that all sets of early stage indices of S(t) are already known.

Suppose that $F_l(\tau)$ disappears at $t_1 > t$ and that no facet disappears at $s \in (t, t_1)$. Then, we set $\mathscr{I}_h(s) = \mathscr{I}_h(t)$ for $s \in (t, t_1)$. We shall construct the set of early stage indices at t_1 as follows. If both F_{l-1} and F_{l+1} do not disappear at t_1 , then we add $\mathscr{I}_{l-1}(t)$, $\mathscr{I}_l(t)$, and $\mathscr{I}_{l+1}(t)$ to the set of early stage indices of a (merged) facet $F_*(t_1)$ containing the limit of $F_{l-1}(s)$ and $F_{l+1}(s)$ as $s \uparrow t_1$. Fig. 11(A) shows an example: At time $t = t_1$, the facet F_4 disappears. Assume that $\mathscr{I}_l(t) = \{l\}$ for $t < t_1$. Then, in this case as shown in Fig. 11(A), $\mathscr{I}_3(t_1) = \{3, 4, 5\}$.

If two consecutive facets F_{l-1} (resp. F_{l+1}) and F_l disappear at t_1 , then we add $\mathcal{I}_l(t)$ to the set of early stage indices of a facet $F_*(t_1)$ containing the limit $F_{l+1}(s)$ (resp. $F_{l-1}(s)$) as $s \uparrow t_1$. Fig. 11(B) shows an example: At $t = t_1$, the facet F_2 and F_3 disappear simultaneously. Assume that $\mathcal{I}_l(t) = \{l\}$ for $t < t_1$. Then, in this case as shown in Fig.11(B), $\mathcal{I}_2(t_1) = \{1, 2\}$ and $\mathcal{I}_3(t_1) = \{3, 4\}$.

By this procedure, the set of early stage indices is uniquely determined for each facet of S(t) as far as S(t) is essentially admissible. (Note that \mathscr{I} is divided into sets of early

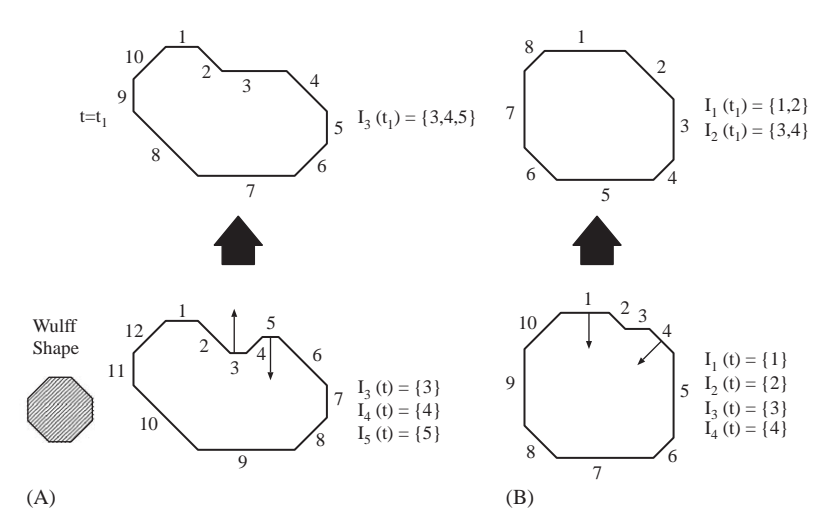


Fig. 11. Construction of indices $\mathcal{I}_I(t)$. (A): A facet $F_4(t)$ disappears at t_1 . (B): Two consecutive facets $F_2(t)$ and $F_3(t)$ disappear simultaneously at $t = t_1$. (We use I instead of \mathscr{I} in this figure. The same convention applies to Figs. 12, 14, 15, and 16.)

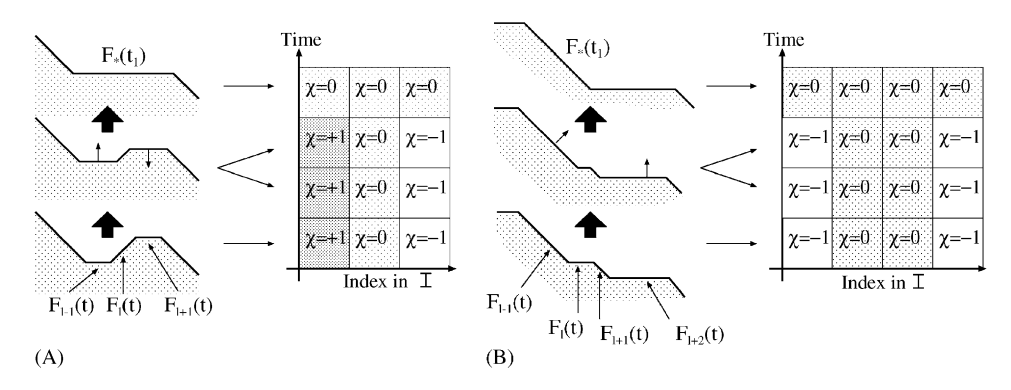


Fig. 12. A scale-space representation of the transition number. It is proved that, if $V = \Lambda_{\gamma}$, then all disappearing facet have zero transition number, and at most two consecutive facets disappear. The *x*-axis represents the index of facet in the early stage contour, and the *y* axis represents the time *t*.

stage indices at t > 0.) Different from Section 2, one facet $F_h(t)$ may have several indices of $\mathcal{I}_h(t)$. Let $\chi(j,t)$ denote the transition number of the facet $F_h(t)$ such that $\mathcal{I}_h(t)$ contains j. As is shown in Fig. 12, the transition number is plot at the corresponding position in the scale-space. This representation is analogous to a usual curvature scale-space.

Fig. 13 presents an example of a crystalline flow numerically obtained with a regular octagon as a Wulff shape. As t increases, the number of (non-trivial) facets in an evolving contour decreases. The evolving polygon becomes an octagon in finite time. When the evolving contour becomes an octagon, the transition numbers of all facets become -1.

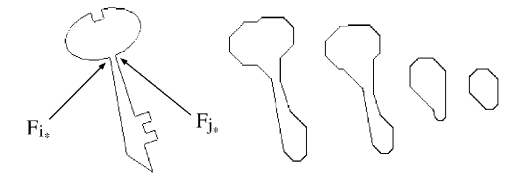


Fig. 13. An example of a crystalline flow. The Wulff shape is a regular octagon.

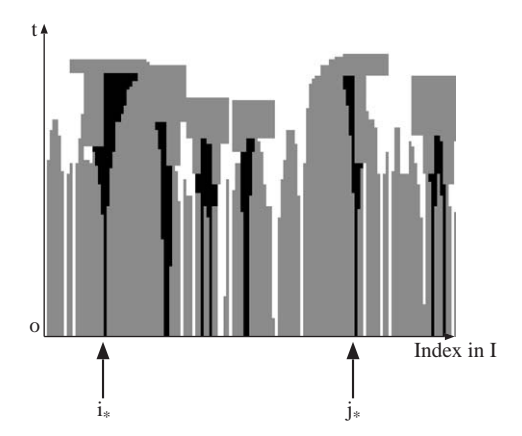


Fig. 14. The scale-space representation that corresponds to Fig. 13. The white area represents $\chi_j = -1$, black one $\chi_j = +1$, and the gray one $\chi_j = 0$. The facets whose indices are i_* and j_* are shown in Fig. 13.

Fig. 14 shows the scale-space representation corresponds to the crystalline shown in Fig. 13. The horizontal axis indicates indices of \mathscr{I} .

Referring to the scale-space representation of the transition number, we extract dominant facets whose transition numbers are not 0 and the values of the transition numbers are inherited for a long time interval in the evolving process. Our algorithm is as follows.

- (1) Make the scale-space representation of the transition number $\chi(j,t)$, where j is in \mathscr{I} and t is the time.
- (2) Divide the scale-space into areas, so that each area has the uniform value of $\chi(j,t)$ inside, and has different value from the neighbouring areas. Let denote such the area as A_k , where $k = 1, 2, \ldots, n$ is the serial number.
- (3) Set the base scale t_0 , and draw a line $t = t_0$ in the scale space. Then, find a set of numbers \mathcal{U}_{t_0} , so that the area A_k contains the line $t = t_0$ and that $\chi(j, t) \neq 0$ on A_k , if $k \in \mathcal{U}_{t_0}$.
- (4) Extract all indices from \mathscr{I} (the set of all indices of early stage contour) that are included in the area $A_k(\tilde{t})$ for some $k \in \mathscr{U}_{t_0}$. Here, $A_k(\tilde{t})$ is the cross-section of A_k at the time \tilde{t} at which $S(\tilde{t})$ is an early stage contour. We call facets of an early stage contour corresponding to such extracted indices *dominant facets* at t_0 . Each of these indices corresponds to a facet of the early stage contour whose transition number is inherited

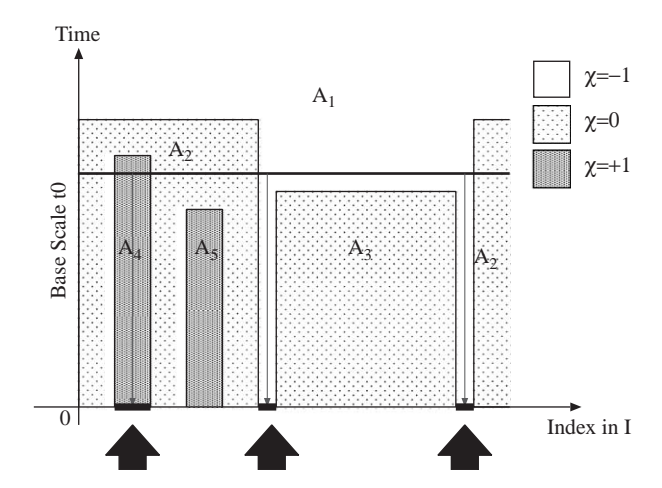


Fig. 15. Dominant facet extraction using the scale-space representation. The facets in an initial contour $\chi \neq 0$ are extracted, if they can be tracked to the base scale t_0 .

to the evolving contour at t_0 . In Fig. 15, the indices of the dominant facets are indicated by up-arrows.

(5) Increase the base scale t_0 by small amount Δt , and repeat (3),(4), and (5), if t_0 is smaller than the scale at which the evolving contour becomes convex (provided that the evolving contour is essentially admissible).

We note that the set of all dominant facets may differ for different base scale t_0 . If $t_0 < t_1$, then, $\mathcal{U}_{t_0} \supseteq \mathcal{U}_{t_1}$. As the result, the number of the dominant facets does not increase as t_0 increases.

Fig. 16 shows an experimental result of dominant facet extraction. The early stage contour has 310 facets. By changing the base scale t_0 , we obtain several sets of dominant facets. Five contours in Fig. 16 are obtained by linking the dominant facets of early stage contour. Although a dominant facet is a segment of finite length, the dominant facets look like black points in Fig. 16 since the length of dominant facets is small. We call such shapes an *extracted contour* at the base scale t_0 . As shown in Fig. 16, fewer facets were extracted for higher value of the base scale. Fig. 17 shows the graph of the number of dominant facets with respect to the change of the base scale. The graph has a staircase pattern. The set of dominant facets which survives in a long interval of base scales yields a typical shape neglecting small details of the original contour.

5. Conclusion

A numerical method for obtaining a crystalline flow starting from a given polygon that is not essentially admissible is presented. The method enables us to use any convex polygon as the Wulff shape. In many cases, a contour in an image is given as a polygon. For example, a contour represented with a chain-code is a polygon that consists of short facets.

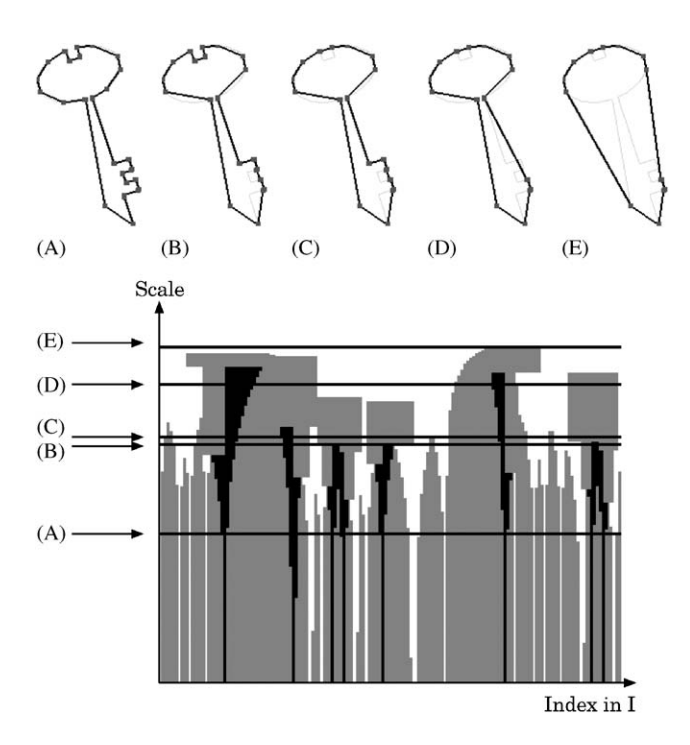


Fig. 16. An experimental result of dominant facet extraction. The corresponding base scales are shown with lines in the scale-space.

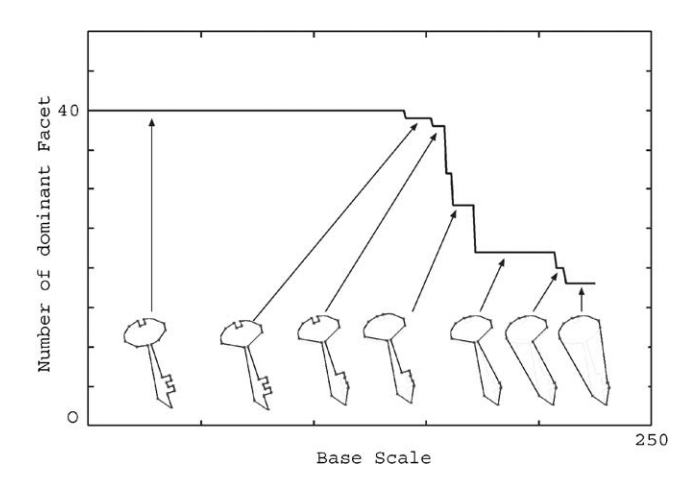


Fig. 17. The change of the dominant facets with respect to the base scale t_0 .

Since the nonlocal curvature Λ_{γ} is determined by the facet length, we can calculate the nonlocal curvature without any numerical approximation. In a crystalline flow, each facet moves with keeping its direction, so it is not difficult to track every facet in scale-space through the evolving process. In particular, it is easy to track the place of a curve where the shape is concave in scale-space compared with other numerical methods approximating conventional curvature flows. We apply a crystalline flow for the multi-scale analysis of a contour figure in an image. We track each facet of an evolving polygon and provide the scale-space representation for a given contour. At several base scales (times), we construct an extracted contour, which are important to represent the shape of a given contour, for example, in image recognition [21]. Note that one is able to take any convex polygon as a Wulff shape. We believe that this freedom is useful for a multi-scale analysis of a contour figure.

Acknowledgements

The authors are grateful for referees for valuable remarks. The second author is grateful to Professor Hitoshi Imai for informative remarks. The third author is partly supported by the Grant in Aid for Scientific Research, No.14204011, No.1563408, the Japan Society for the Promotion of Science(JSPS). This work is also supported by COE 'Mathematics of Nonlinear Structure via Singularities' of JSPS.

References

- [1] L. Alvarez, F. Guichard, Axioms and fundamental equations of image processing, Arch. Rational Mech. Anal. 123 (1993) 199–257.
- [2] S.B. Angenent, M.E. Gurtin, Multiphase thermomechanics with interfacial structure 2. Evolution of an isothermal interface, Arch. Rational Mech. Anal. 108 (1989) 323–391.
- [3] R.W. Brockett, P. Maragos, Evolution equations for continuous scale morphology, Proceedings of the IEEE International Conference on Acoustics Speech, Signal Processing, San Francisco, LA, March 1992.
- [4] F. Cao, Geometric Curve Evolution and Image Processing, Lecture Notes in Mathematics, vol. 1805, Springer, Berlin, 2003.
- [5] Y.-G. Chen, Y. Giga, S. Goto, Uniqueness and existence of viscosity solutions of generalized mean curvature flow equations, J. Differential Geom. 33 (1991) 749–786.
- [6] L.C. Evans, J. Spruck, Motion of level-sets by mean curvature, I, J. Differential Geom. 33 (1991) 635-681.
- [7] Y. Giga, A level set method for surface evolution equations, Sugaku 47 (1993) 321–340 Eng. translation, Sugaku Exposition 10 (1995) 217–241.
- [8] M.-H. Giga, Y. Giga, Consistency in evolutions by crystalline curvature, in: M. Niezgodka, P. Strzelecki (Eds.), Free Boundary Problems '95, Theory and Applications, Proceedings of the Zakopane Congress, Poland, 1995, pp. 186–202.
- [9] M.-H. Giga, Y. Giga, Crystalline and level-set flow—convergence of a crystalline algorithm for a general anisotropic curvature flow in the plane, in: N. Kenmochi (Ed.), Free Boundary Problems: Theory And Applications I, Gakuto International Series in Mathematical Sciences and Applications, vol. 13, 2000, pp. 64–79.
- [10] M.-H. Giga, Y. Giga, Generalized motion by nonlocal curvature in the plane, Arch. Rational Mech. Anal. 159 (2001) 295–333.
- [11] M.-H. Giga, Y. Giga, H. Hontani, Selfsimilar solutions in motion of curves by crystalline energy, Minisymposium Lecture of 5th International Congress on Industrial and Applied Mathematics, Sydney, 2003, July.

- [12] M.-H. Giga, Y. Giga, H. Hontani, Selfsimilar expanding solutions in a sector for a crystalline flow, preprint.
- [13] Y. Giga, S. Goto, Motion of hypersurfaces and geometric equations, J. Math. Soc. Japan 44 (1992) 99-111.
- [14] M.E. Gurtin, Thermomechanics of Evolving Phase Boundaries in the Plane, Oxford, Clarendon Press, 1993.
- [15] H. Hontani, K. Deguchi, Multi-scale image analysis for detection of characteristic component figure shapes and sizes, Proceedings of 14th International Conference on Pattern Recognition, 1998, pp. 1470–1472.
- [16] H. Hontani, K. Deguchi, Introducing a crystalline flow for a contour figure analysis, IEICE Trans. (D) Information and System E86-D (7) (2003) 1198–1205.
- [17] H. Hontani, M.-H. Giga, Y. Giga, K. Deguchi, A computation of a crystalline flow starting from non-admissible polygon using expanding selfsimilar solutions, 11th International Conference DGCI 2003, Lecture Notes Computer Sciences, vol. 2886, Springer, Naples, 2003, pp. 465–474.
- [18] B.B. Kimia, A.R. Tannenbaum, S.W. Zucker, Shapes, shocks, and deformations I: the components of twodimensional shape and the reaction-diffusion space, Internat. J. Comput. Vision 15 (1995) 189–224.
- [19] J.J. Koenderink, The structure of images, Biol. Cybern. 50 (1984) 363-370.
- [20] T. Lindeberg, Scale-Space Theory in Computer Vision, Kluwer Academic Publishers, Dordrecht, 1994.
- [21] D. Marr, Vision, Freeman (1982) 20-22.
- [22] F. Mokhtarian, A. Mackworth, A theory of multiscale, curvature-based shape representation for planner curves, IEEE Trans. Pattern Anal. Mach. Intell. 14 (8) (1992) 789–805.
- [23] S. Osher, J.A. Sethian, Fronts propagating with curvature-dependent speed: algorithms based on Hamilton–Jacobi formulations, J. Comput. Phys. 79 (1988) 12–49.
- [24] A. Rattarangsi, R.T. Chin, Scale-based detection of corners of planar curves, IEEE Trans. Pattern Anal. Mach. Intell. 14 (4) (1992) 430–449.
- [25] G. Sapiro, R. Kimmel, D. Shaked, B.B. Kimia, A.M. Bruckstein, Implementing continuous-scale morphology via curve evolution, Pattern Recognition 26 (9) (1993) 1363–1372.
- [26] J. Taylor, Constructions and conjectures in crystalline nondifferential geometry, Proceedings of the Conference on Differential Geometry, vol. 52, Pitman, London, 1991, pp. 321–336.
- [27] A.P. Witkin, Scale space filtering: a new approach to multi-scale descriptions, Proceedings of 8th International Joint Conference of Artificial Intelligence, 1983, pp. 1019–1022.